

Access this article online
Quick Response Code:

Website: http://journals.lww.com/TJOP
DOI: 10.4103/tjo.TJO-D-24-00066

# Utility of multimodal imaging in the clinical diagnosis of inherited retinal degenerations

Brian J. H. Lee<sup>1</sup>, Christopher Z. Y. Sun<sup>1,2</sup>, Charles J. T. Ong<sup>1,2</sup>, Kanika Jain<sup>3</sup>, Tien-En Tan<sup>1,2</sup>, Choi Mun Chan<sup>1,2</sup>, Ranjana S. Mathur<sup>1,2</sup>, Rachael W. C. Tang<sup>1</sup>, Yasmin Bylstra<sup>4</sup>, Sylvia P. R. Kam<sup>5</sup>, Weng Khong Lim<sup>4,6,7,8</sup>, Beau J. Fenner<sup>1,2\*</sup>

## Abstract:

Inherited retinal degeneration (IRD) is a heterogeneous group of genetic disorders of variable onset and severity, with vision loss being a common endpoint in most cases. More than 50 distinct IRD phenotypes and over 280 causative genes have been described. Establishing a clinical phenotype for patients with IRD is particularly challenging due to clinical variability even among patients with similar genotypes. Clinical phenotyping provides a foundation for understanding disease progression and informing subsequent genetic investigations. Establishing a clear clinical phenotype for IRD cases is required to corroborate the data obtained from exome and genome sequencing, which often yields numerous variants in genes associated with IRD. In the current work, we review the use of contemporary retinal imaging modalities, including ultra-widefield and autofluorescence imaging, optical coherence tomography, and multispectral imaging, in the diagnosis of IRD.

## Keywords:

Autofluorescence, imaging, inherited retinal degeneration, inherited retinal disease, optical coherence tomography, retina

## Introduction

Inherited retinal degeneration (IRD) refers to a heterogeneous group of genetic disorders of variable onset and severity, with vision loss being a common endpoint in most cases. More than 50 distinct IRD phenotypes and over 280 causative genes have been described.<sup>[1]</sup> However, in many regional cohort studies, more than half of the IRD cases are retinitis pigmentosa (RP, or rod-cone dystrophy),<sup>[2]</sup> with cone and cone-rod dystrophies (CRDs), and Stargardt macular dystrophy also making significant contributions to the overall IRD burden. Contemporary estimates of IRD prevalence in the general population range from approximately 1 in 1000 to 1 in 2000.<sup>[2-9]</sup> Unlike more prevalent retinal diseases such

as age-related macular degeneration (AMD) and retinal vein occlusion, IRDs have a disproportionate impact on working-age adults, leading to significant impacts on economic productivity.<sup>[2,10,11]</sup> IRD has been reported as the most common cause of blindness among working-age adults in nations with sufficiently well-developed health-care systems, overtaking diabetic retinopathy (DR) due to advances in screening and management of the latter.<sup>[10,11]</sup>

IRD can be broadly classified based on the disease entity: (1) photoreceptor dystrophies, (2) macular dystrophies, (3) chorioretinal dystrophies, (4) inherited vitreoretinopathies, (5) metabolic retinopathies, and (6) others [Table 1]. Establishing a clinical phenotype for patients with IRD is particularly challenging due to clinical variability even among patients with similar genotypes.<sup>[12-14]</sup> Early

This is an open access journal, and articles are distributed under the terms of the Creative Commons Attribution-NonCommercial-ShareAlike 4.0 License, which allows others to remix, tweak, and build upon the work non-commercially, as long as appropriate credit is given and the new creations are licensed under the identical terms.

For reprints contact: WKHLRPMedknow\_reprints@wolterskluwer.com

**How to cite this article:** Lee BJ, Sun CZ, Ong CJ, Jain K, Tan TE, Chan CM, et al. Utility of multimodal imaging in the clinical diagnosis of inherited retinal degenerations. Taiwan J Ophthalmol 2024;14:486-96.

<sup>1</sup>Singapore National Eye Centre, Singapore Eye Research Institute, <sup>2</sup>Ophthalmology and Visual Sciences Clinical Academic Program, Duke-NUS Graduate Medical School, <sup>3</sup>Genome Institute of Singapore, <sup>4</sup>SingHealth-Duke-NUS Genomic Medicine Centre, Institute of Precision Medicine, <sup>5</sup>Department of Paediatrics, KK Women's and Children's Hospital, <sup>6</sup>SingHealth Duke-NUS Genomic Medicine Centre, <sup>7</sup>Cancer and Stem Cell Biology Program, Duke-NUS Medical School, <sup>8</sup>Genome Institute of Singapore, Agency for Science, Technology and Research, Singapore

### \*Address for correspondence:

Dr. Beau J. Fenner,  
Department of Medical Retina, Singapore National Eye Centre, 11 Third Hospital Avenue, 168751 Singapore.  
E-mail: beaufenner@duke-nus.edu.sg

Submission: 14-06-2024  
Accepted: 25-08-2024  
Published: 03-12-2024

**Table 1: Typical imaging findings for selected inherited retinal degenerations**

Group	Phenotype	Fundoscopy findings	OCT findings	AF findings	Associated genes
Photoreceptor dystrophies	RP	Bone-spicule pigmentation, attenuated retinal vessels, nummular RPE atrophy in late stages	Parafoveal loss of EZ band	Hyperautofluorescent rings, peripheral hypoafluorescence	<i>EYS, RPGR, RHO, USH2A, PRPF31, EYS</i> , etc.
	CRD	Bull's eye maculopathy, macular atrophy	Foveal EZ loss	Foveal and macular hypoafluorescence	<i>CRX, GUCY2D, RPGR</i> etc.
	LCA	Often unremarkable in early stage; eventually progressing to peripheral pigmentary changes	Variable; often have parafoveal EZ loss; retinal thickening and schisis-like changes in <i>CRB1</i> disease	Diffuse hypoafluorescence	<i>GUCY2D, CRB1, RPE65, AIPL1</i> , etc.
	ESCS	Whiteish nummular deposits around macular arcades, progressing to extensive peripheral atrophy with pigment changes	Patchy losses of the RPE and EZ bands; schisis-like changes that can mimic XLRS	Paramacular hyperautofluorescent nummular lesions	<i>NR2E3</i>
	CSNB	Normal to mild fundus changes	Typically, normal in appearance	Normal to mild changes	<i>NYX, CACNA1F, GRM6, TRPM1</i> , etc.
Macular dystrophies	Best vitelliform macular dystrophy	Yellowish vitelliform lesions; may be unifocal or multifocal	Subretinal vitelliform deposits, subretinal fluid; often complicated by secondary type 2 CNV membranes	Hyperautofluorescent central lesion with heterogenous signals	<i>BEST1, IMPG2</i>
	STGD	Highly variable; adolescents typically have pisciform flecks and central macular atrophy	Highly variable; commonly central EZ loss but may have selective foveal preservation	Central hypoafluorescence matching atrophy; may have hyperautofluorescent flecks	<i>ABCA4</i>
	Sorsby fundus dystrophy	Subretinal neovascularization, choroidal thinning	Outer retinal atrophy, subretinal hyper-reflective material in areas of CNV, with subretinal fibrosis	Hypoafluorescence in areas of atrophy	<i>TIMP3</i>
	North carolina macular dystrophy	Highly variable; classically with central coloboma-like macular excavation with gliotic rim	Highly variable; classically with chorioretinal excavation and loss of retinal laminations	Mixed AF signals	<i>MCDR1</i>
Chorioretinal dystrophies	CHM	Chorioretinal atrophy, peripheral pigmentary changes	Subretinal deposits, outer retinal layer loss and marked choroidal thinning	Hypoafluorescence corresponding to atrophy	<i>CHM</i>
	Bietti crystalline dystrophy	Crystalline deposits in early stages, progressing to posterior pole chorioretinal atrophy	EZ and RPE losses and frequent outer retinal tubulations	Areas of hypoafluorescence matching atrophy	<i>CYP4V2</i>
Inherited vitreoretinopathies	FEVR	Peripheral retinal avascularity like retinopathy of prematurity; retinal neovascularization	Often unremarkable macular OCT findings; neurosensory detachment as a complication	Peripheral hypoafluorescence on UWF imaging	<i>NDP, FZD4, LRP5, TSPAN12</i> , etc.
Metabolic retinopathies	Batten disease	Pigmentary retinopathy, optic nerve atrophy	Extensive EZ loss and loss of inner retinal laminations	Mixed AF signals	<i>CLN1, CLN3, CLN5</i> etc.
	Gyrate atrophy	Chorioretinal atrophy with scalloped borders, progressing toward posterior pole late in disease	Subretinal deposits, retinal thinning and loss of EZ band	Hypoafluorescence in areas of chorioretinal atrophy	<i>OAT</i>
Other inherited retinal diseases	XLRS	Radial spoke-like cysts in macula	Variable; typically, with inner retinal schisis and foveal EZ loss late in disease	Mixed AF signals	<i>RS1</i>

RP=Retinitis pigmentosa, CRD=Cone-rod dystrophy, AF=Autofluorescence, LCA=Leber congenital amaurosis, ESCS=Enhanced S-cone syndrome, CSNB=Congenital stationary night blindness, STGD=Stargardt macular dystrophy, CHM=Choroideremia, FEVR=Familial exudative vitreoretinopathy, XLRS=X-linked retinoschisis, UWF=Ultra-widefield, EZ=Ellipsoid zone, OCT=Optical coherence tomography, CNV=choroidal neovascularisation

classifications of IRD phenotypes were descriptive, relying on observable clinical features and progression patterns. Pioneering works by Franceschetti and Dieterle in the mid-20<sup>th</sup> century categorized RP based on fundus appearance and visual field loss.<sup>[15]</sup> This approach was expanded to incorporate electroretinography

findings to differentiate between rod-cone and CRDs.<sup>[16,17]</sup> Accurate clinical phenotyping in these early classifications provided a foundation for understanding disease progression and informing subsequent genetic investigations. In the current practice, establishing a clear clinical phenotype for IRD cases is required to

corroborate the data obtained from genetic testing using the next-generation sequencing, which often yields many variants of uncertain significance in genes associated with IRD.

Recognizing the global disease burden due to IRD, there are ongoing efforts to develop molecular therapeutics targeting common disease-causing IRD genes or variants. These include gene augmentation with adeno-associated virus vectors, DNA and RNA editing with CRISPR or adenosine deaminase acting on RNA,<sup>[18]</sup> and oligonucleotide-mediated knockdown or exon skipping, all delivered through surgical or clinic-based procedural approaches.<sup>[19,20]</sup> The implications of inappropriate and invasive interventions for patients in whom the genetic diagnosis is incorrectly established highlight the importance of reliable clinical phenotyping to strengthen the conclusions made from genetic testing. IRD diagnosis is now more heavily dependent on retinal imaging than previously, and a small number of key imaging modalities can be combined with clinical history to reliably establish a phenotype in the majority of IRD cases.<sup>[13]</sup> In the current work, we reviewed the key retinal imaging modalities that are used in contemporary clinical practice for the clinical diagnosis and management of IRD.

## Fundus Photography

Accurate documentation of clinical findings with color fundus photography (CFP) at initial presentation is extremely useful in IRD as the fundus appearance changes with time in many of the clinical phenotypes.

The classical pisciform flecks of typical Stargardt disease [Figure 1a], which may be prominent earlier in the disease, resorb with time and the late-stage atrophy may be mistaken for other pathology like geographic atrophy secondary to AMD. Similarly, progressive RPE atrophy in Bietti's crystalline dystrophy decreases the visibility of the characteristic crystalline deposits in the macula and midperiphery due to increased paleness of light reflected from the fundus which can mask the retinal crystals<sup>[21]</sup> [Figure 1b]. Standard field (30°–50°) CFP is noncontact, relatively inexpensive, fast, and provides a true color image of the retina. However, there are limitations to conventional CFP, including a limited visual angle of 30°–50° due to its method of illumination through the annulus of the pupil, which is restricted in the undilated pupil.<sup>[22]</sup>

Ultra-widefield (UWF) FP provides a visual angle of up to 200°, reducing the possibility of missed lesions in the peripheral retina beyond what is usually captured using conventional CFP, even without pharmacologic pupillary dilation.<sup>[23]</sup> Currently, the most commonly utilized UWF-FP systems available are Clarus (Carl Zeiss Meditec, Jena, Germany) and Optos cameras (Optos, MA, USA).<sup>[24]</sup> Evaluation of the retina with UWF-FP is especially beneficial in IRDs that manifest in the peripheral retina such as choroideremia, gyrate atrophy, retinitis pigmentosa, and X-linked retinoschisis [Figure 1c and d].<sup>[25]</sup> Similarly, the extent of pigmentary changes and vessel attenuation are better appreciated on UWF-FP [Figure 1e].<sup>[25]</sup> Currently, most studies on the clinical application of UWF-FP are focused

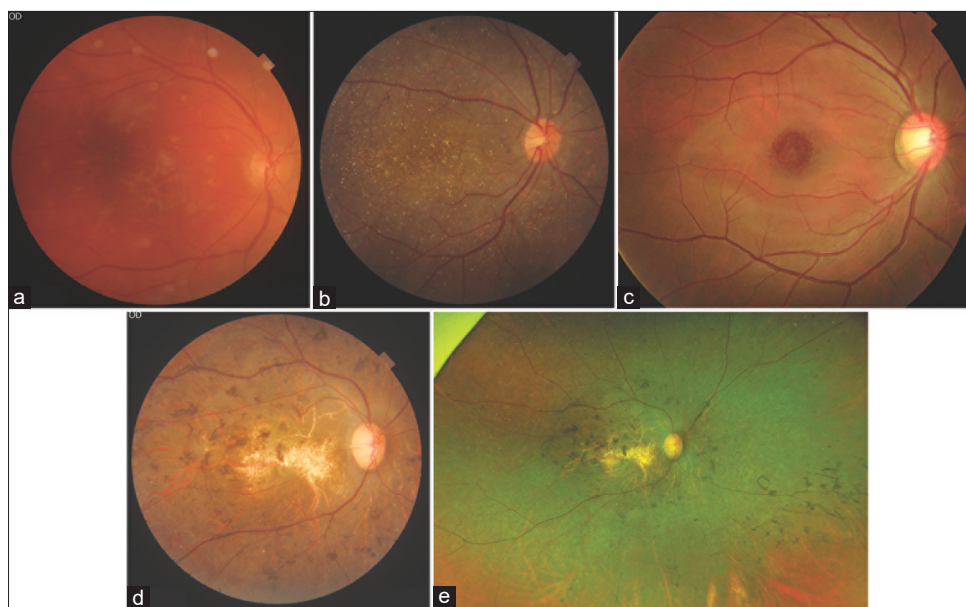


**Figure 1:** Conventional and ultra-widefield fundus photography. (a) Retinal flecks are prominently seen in this 61-year-old male with ABCA4-associated Stargardt macular dystrophy. (b) Crystalline deposits throughout the macula in a 26-year-old female with Bietti crystalline dystrophy due to biallelic mutations in CYP4V2. (c) Radial spoke-like cysts in a 15-year-old male with X-linked retinoschisis secondary to pathogenic mutations in RS1. (d) Diffuse retinal atrophy mimicking RP with bone spicule-like pigmentation in a 37-year-old female with severe early-onset ABCA4-associated retinal degeneration. (e) UWF pseudocolor imaging (Optos) revealed that atrophy was more prominent at the macula and posterior pole, with sparing of the peripheries. This is typical of ABCA4-associated macular dystrophy but less common in RP



on DR populations but there is a window of opportunity for novel research into its application for IRDs as well. For example, Antaki *et al.* showed that an automated machine-learning model could detect RP from UWF-FP images with high diagnostic accuracy.<sup>[26]</sup>

## Autofluorescence Imaging

Fundus autofluorescence (AF) has arguably become the most important imaging modality in the contemporary assessment of IRD. It highlights the areas of RPE dysfunction and atrophy that may not be clinically apparent on slit-lamp biomicroscopy or CFP. Hyper-AF signals are prominently visible in areas of lipofuscin accumulation such as in *ABCA4*-associated retinal degeneration [Figure 2a and b], macrophage infiltration in *NR2E3*-associated retinal degeneration [Figure 2c and d]<sup>[27]</sup> and lipofuscin accumulation in vitelliform macular dystrophy [Figure 2e and f]. Hypoautofluorescence can be seen in areas of atrophy such as retinitis pigmentosa, choroideremia, and gyrate atrophy.<sup>[28]</sup> Previously, standard field AF, on platforms such as the Heidelberg Spectralis, was the most

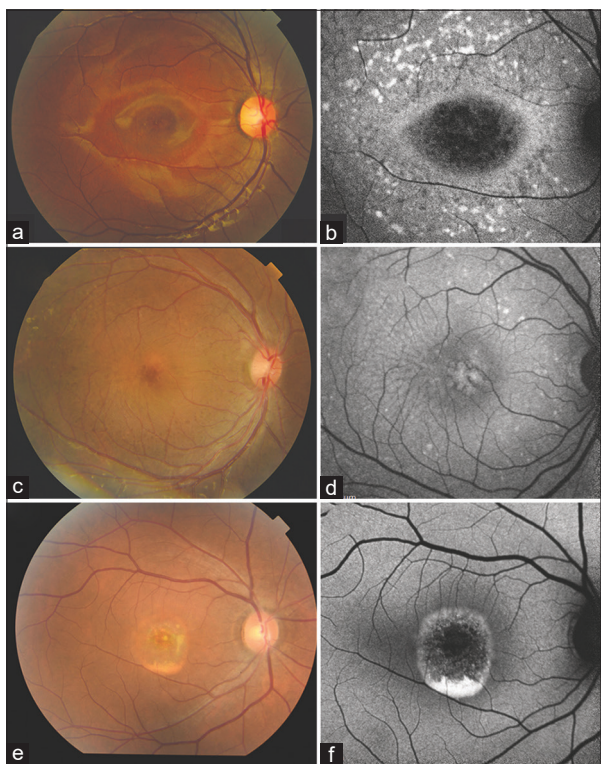


**Figure 2:** Fundus autofluorescence in cases of IRD. (a) Macular atrophy and flecks in a 13-year-old male with *ABCA4*-associated macular dystrophy; (b) fundus AF imaging of the same patient highlights the atrophy with a central elliptical focus of hypoautofluorescence surrounded by hyperautofluorescent flecks. (c) Cystoid macular degeneration and peripheral nummular deposits in a 16-year-old male with *NR2E3*-associated retinopathy; (d) fundus AF imaging highlights the cystic spaces and peripheral hyperautofluorescent nummular lesions in the peripheral macula. (e) A classical pseudohypopyon appearance in a 40-year-old male with autosomal dominant Best disease; (f) macular autofluorescence highlights the vitelliform material with inferior gravitational 'fluid' level.

common imaging tool for IRDs but was restricted to a visual angle of 30°–50°.<sup>[29]</sup> UWF-AF, particularly with Optos cameras, has become one of the most important imaging modalities for diagnosing and monitoring IRD, especially in peripheral retinopathies such as RP and choroideremia [Figure 2c and d]. Hyperautofluorescent rings on AF imaging are common in RP,<sup>[30]</sup> with a central hypoautofluorescent bulls-eye-like pattern of maculopathy.<sup>[31]</sup> *EYS*-associated RP in particular is associated with seemingly genotype-specific AF patterns. For example, a study by Sengillo *et al.* described crescent-shaped and typical hyperautofluorescent rings to be associated with variants in the C-terminal one-third of the *EYS* protein while the absence of an autofluorescent ring suggested variants in the amino-terminus.<sup>[31]</sup> These serve as a valuable biomarker that aids in the formulation of genetic hypotheses during initial patient workup.<sup>[31,32]</sup> Particularly in East Asia, where *EYS*-associated RP is among the most prevalent causes of IRD, a clinical suspicion of *EYS* can direct follow-up genetic testing where patients are initially found to have an incomplete genotype with a single *EYS* variant and a missing second variant. In the presence of atypical patterns of fundus AF, a clinician may spend additional resources such as genome or long-read sequencing to identify a second disease-causing variant.

Aside from clinical diagnosis, AF is commonly used to monitor disease progression in IRD. Metabolic stress from photoreceptor degeneration leads to the accumulation of lipofuscin in the RPE, which appears hyperautofluorescent and progression to RPE atrophy leads to AF signal loss hypoautofluorescence.<sup>[33]</sup> In Best vitelliform macular dystrophy, AF patterns demonstrate passage from the pre-atrophic vitelliform stages [Figure 2e and f] through to the atrophic stage of the disease. It is increasingly appreciated that specific AF patterns can be used to predict IRD genotypes. Patal *et al.* demonstrated that macular abnormalities in fundus AF differentiated between autosomal recessive RP caused by *FAM161A*, *DHDDS*, or *MAK* genes in terms of the pattern of macular abnormalities, as well as the configuration and extent of the hypoautofluorescence. Specifically for *DHDDS*, a more abnormal AF pattern of the macular and extensive peripheral hypoautofluorescence were observed.<sup>[34]</sup>

Despite the aforementioned advantages, FAF remains a supplementary imaging modality in many IRDs where AF often represents the pathological epiphenomenon. Furthermore, the autofluorescent signals are highly variable depending on refractive error, lipofuscin content and genetic expression during the ageing process. Hence, it is challenging to produce a reference database to consistently classify IRDs based on the FAF findings.<sup>[28]</sup>

## Optical Coherence Tomography and Optical Coherence Tomography-angiography

Optical coherence tomography (OCT) is a noninvasive imaging modality that allows for a detailed cross-sectional analysis of the retina by measuring the echo time delay and magnitude of backscattered light.<sup>[35]</sup> Since its first iteration in the 1990s, OCT has been progressively enhanced which has led to the development of spectral domain and swept source modalities with faster image acquisition and higher resolution than historical time-domain OCT instruments.<sup>[36]</sup> Like fundus AF, OCT imaging has become a cornerstone technology for the diagnosis and management of IRD.

A hallmark of RP, along with its characteristic bone spicule-like pigmentation and arteriolar attenuation visible on CFP and UWF-CFP, is paracentral ellipsoid zone (EZ) loss and macular photoreceptor thinning visible on OCT [Figure 3a].<sup>[37,38]</sup> The EZ changes on OCT are a reliable marker of visual acuity and disease progression, while cystoid macular edema complicating RP is easily observable on OCT imaging.<sup>[39]</sup> In Best disease and other macular dystrophies, OCT is an essential imaging modality for the detection and management of secondary choroidal neovascularization [Figure 3b].<sup>[40,41]</sup> Foveal schisis and peripheral retinoschisis, which are key diagnostic features of X-linked retinoschisis, are easily visualized on OCT and this enables rapid and highly sensitive screening of family members in addition to

disease monitoring for affected individuals.<sup>[42,43]</sup> OCT can aid with early diagnosis of IRD for individuals with grossly normal fundus findings such as LCA, which can sometimes present with early and severe visual loss accompanied by loss of the outer retinal layers [Figure 3c].<sup>[44]</sup> Macular OCT imaging of individuals with *CRB1*-associated LCA demonstrates an essentially pathognomonic finding of prominent retinal thickening and disorganization which is distinct from the more typical EZ loss with normal inner retinal structure in early LCA cases with other genotypes.<sup>[45,46]</sup> Photoreceptor outer segment shortening (OS) is one of the earliest findings in rod-cone dystrophy and can be assessed by measuring the length between the EZ layer and the RPE, and shortening of the photoreceptor OS is shown to significantly correlate with several functional parameters such as visual field, central retinal sensitivity, and visual acuity.<sup>[47-50]</sup> The relevance of OCT in diagnosing IRDs is also shown in the distinction of systemic diseases such as neuronal ceroid lipofuscinosis (CLN) associated retinal degenerations such as Batten disease from *ABCA4*-associated retinal degeneration, where loss of inner retinal lamination which is seen in CLN diseases but not in the latter [Figure 3d].<sup>[46]</sup>

OCT angiography enables visualization of the retinal vasculature by capturing consecutive A-scans at the same location of the retina which are separated by a brief lapse in time. The decorrelation signal, which is the difference between signals of two A-scans, is interpreted

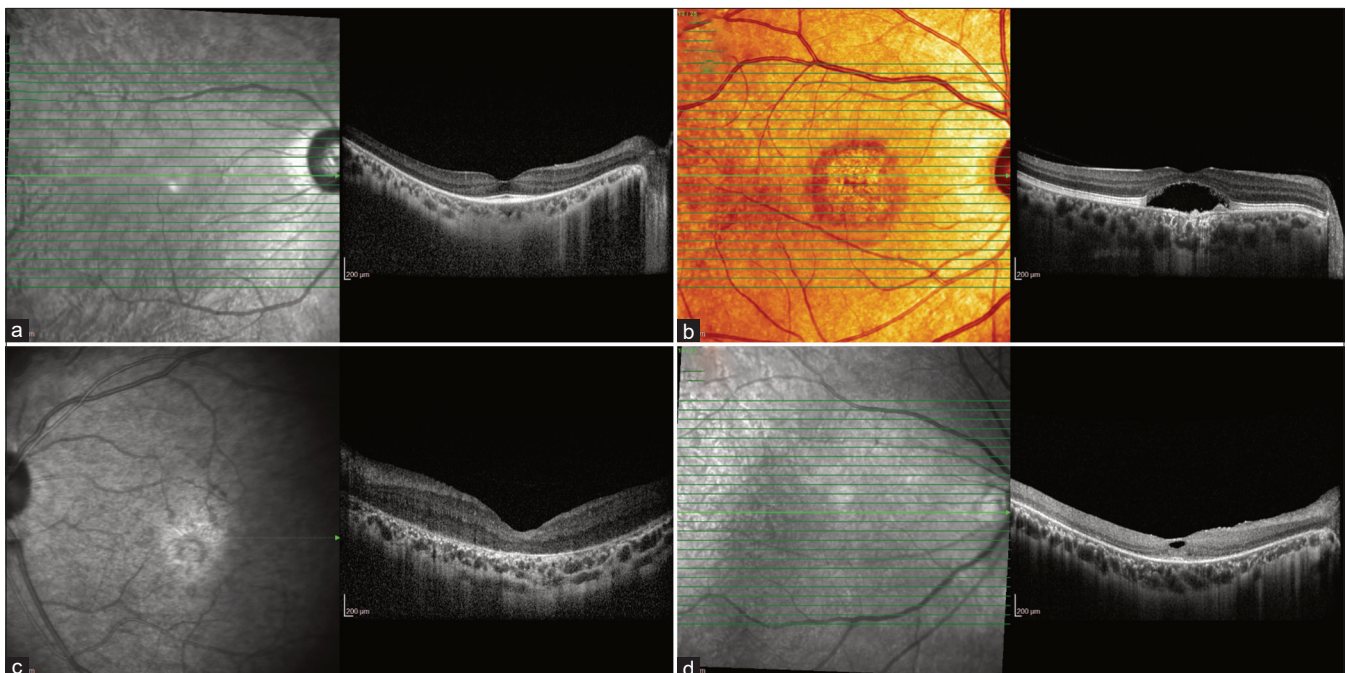


**Figure 3:** Spectral domain optical coherence tomography imaging in Inherited retinal degeneration. (a) Paracentral ellipsoid zone (EZ) band loss in a 25-year-old male with *RHO*-associated RP. (b) Subfoveal fluid with elongated photoreceptor outer segments in a 40-year-old male with dominantly inherited Best vitelliform macular dystrophy secondary to a pathogenic *BEST1* variant. (c) Diffuse outer retinal losses and prominent retinal thickening in a 7-year-old male with *CRB1*-associated LCA. (d) Loss of inner retinal laminations, cystoid foveal changes and parafoveal EZ loss in a 26-year-old female with *CLN1*-associated retinal degeneration



as being due to motion, and in the case of the retina, the blood flow as the retina is static.<sup>[51]</sup> It is a faster and safer method of assessing retinal vasculature compared to conventional intravenous fluorescein and indocyanine green (ICG) angiography, although in current practice, its use is mainly limited to pathologies of the macula and posterior pole.<sup>[52]</sup> OCT-A is commonly employed for the detection and monitoring of secondary CNV in macular dystrophies,<sup>[53]</sup> although recent studies have demonstrated lower vascular flow and densities of superficial and deep retinal capillary plexuses in RP patients compared to controls, and this was significantly associated with visual acuity.<sup>[54-56]</sup> Moreover, OCT-A has been used to demonstrate quantitative differences in microvascular parameters over time, with decreasing capillary plexus densities and choroidal vascularity indexes in RP patients.<sup>[57]</sup> An enlarged foveal avascular zone has been reported in Stargardt and Best disease, which are the potential predictors of visual function.<sup>[58]</sup> A comparison of the relative diagnostic utility of commonly employed retinal imaging modalities, namely standard and UWF fundus photography, standard and UWF AF, and macular OCT, applied to typical IRD phenotypes, is provided in Figure 4.

### Fluorescein Angiography and Indocyanine Green Angiography

Conventional intravenous dye angiography with fluorescein and ICG, although more invasive than OCT-A, enables visualization of vascular leakage and thus assessment of the integrity of the blood-retinal barrier.<sup>[59]</sup> With the widespread adoption of OCT-A into clinical practice in many centers, conventional angiography is less commonly employed for routine IRD management, although UWF angiography is particularly useful for IRDs associated with vascular abnormalities. Vasoproliferative lesions are a relatively common finding in patients with RP and are often peripherally located [Figure 5].<sup>[41,60]</sup> In such cases, UWF angiography can assist with clinical diagnosis and direct treatment strategies with laser photocoagulation.

### Multispectral Imaging

Multispectral imaging (MSI) is a novel imaging system that uses nonoverlapping discrete spectral bands to highlight specific features within the field of view that are already employed in various fields such as biochemistry, weather forecasting, and military applications.<sup>[61]</sup> In clinical ophthalmology, MSI allows the visualization of a spectrum of retinal and choroidal pathologies including early RPE and retinovascular changes that may not be apparent clinically or with conventional fundus imaging.<sup>[62]</sup> In phenotyping inherited retinal diseases such as Stargardt disease, blue reflectance [450–490 nm;

Figure 6c and g] is valuable for detecting outer retinal changes, particularly lipofuscin accumulation and RPE abnormalities, making it useful for identifying early disease features that might not yet appear on AF. Green reflectance [500–570 nm; Figure 6d and h] enhances the contrast of the macula and middle retinal layers, providing better visualization of vascular and RPE changes, while infrared reflectance [600–700 nm; Figure 6b and f] penetrates deeper, offering insights into choroidal structure and highlighting areas of retinal atrophy. Compared to AF, which focuses on metabolic changes, multispectral reflectance imaging excels at providing complementary structural information, particularly in early disease detection and assessing deeper retinal and choroidal involvement. A study on the use of MSI in choroideremia by Dugel *et al.*<sup>[63]</sup> found RPE mottling with melanin clumping that was not seen with OCT and fundus AF. Similarly, MSI can be employed to evaluate flecks seen in *ABCA4*- and *PRPH* 2-associated retinal degenerations [Figure 6a and e]. Currently, there are ongoing clinical trials on stem cell therapy, gene therapy and medical therapy that are in the early trial phases for Stargardt disease.<sup>[64]</sup> However, knowledge of the RPE atrophy expansion rate depicted as the areas of hypoautofluorescence on fundus AF is crucial to guide these trials, as in the ProgStar study.<sup>[65]</sup> Currently, AF and UWF-AF are commonly used to monitor atrophy in Stargardt disease as they are relatively fast and noninvasive imaging modalities.<sup>[66]</sup> The advantages of MSI over FAF include its ability to potentially detect earlier non-lipofuscin abnormalities before the RPE changes become apparent as well as visualization of subtle flecks that may not be seen in other imaging modalities [Figure 6b].<sup>[62,67]</sup>

### Adaptive Optics

Adaptive optics (AO) was initially used in astronomical telescopes to correct for atmospheric distortion.<sup>[68]</sup> AO works using a wavefront sensor and deformable mirror to measure and correct for ocular aberrations, which allows for high-resolution imaging of a cellular layer including individual photoreceptor cells, ganglion cells, and RPE.<sup>[68,69]</sup> This is especially useful in IRD where the predominant pathology is often in the photoreceptor layer, such as in CRDs.<sup>[70]</sup> Duncan *et al.* reported significantly different cone spacing values for CRD and RP patients from healthy individuals using AO-SLO imaging, with cone spacing increased in all CRD patients, even in those with early disease.<sup>[68,71]</sup> Another study by Nakatake *et al.* found that AO-SLO could detect areas of decreased cone density in RP patients with preserved parafoveal EZ bands on OCT.<sup>[70]</sup> Enhanced S-cone syndrome, caused by mutations in *NR2E3*, can also be identified using AO from its characteristic retinal mosaic asymmetry due to an excess of S-cones.<sup>[72,73]</sup>

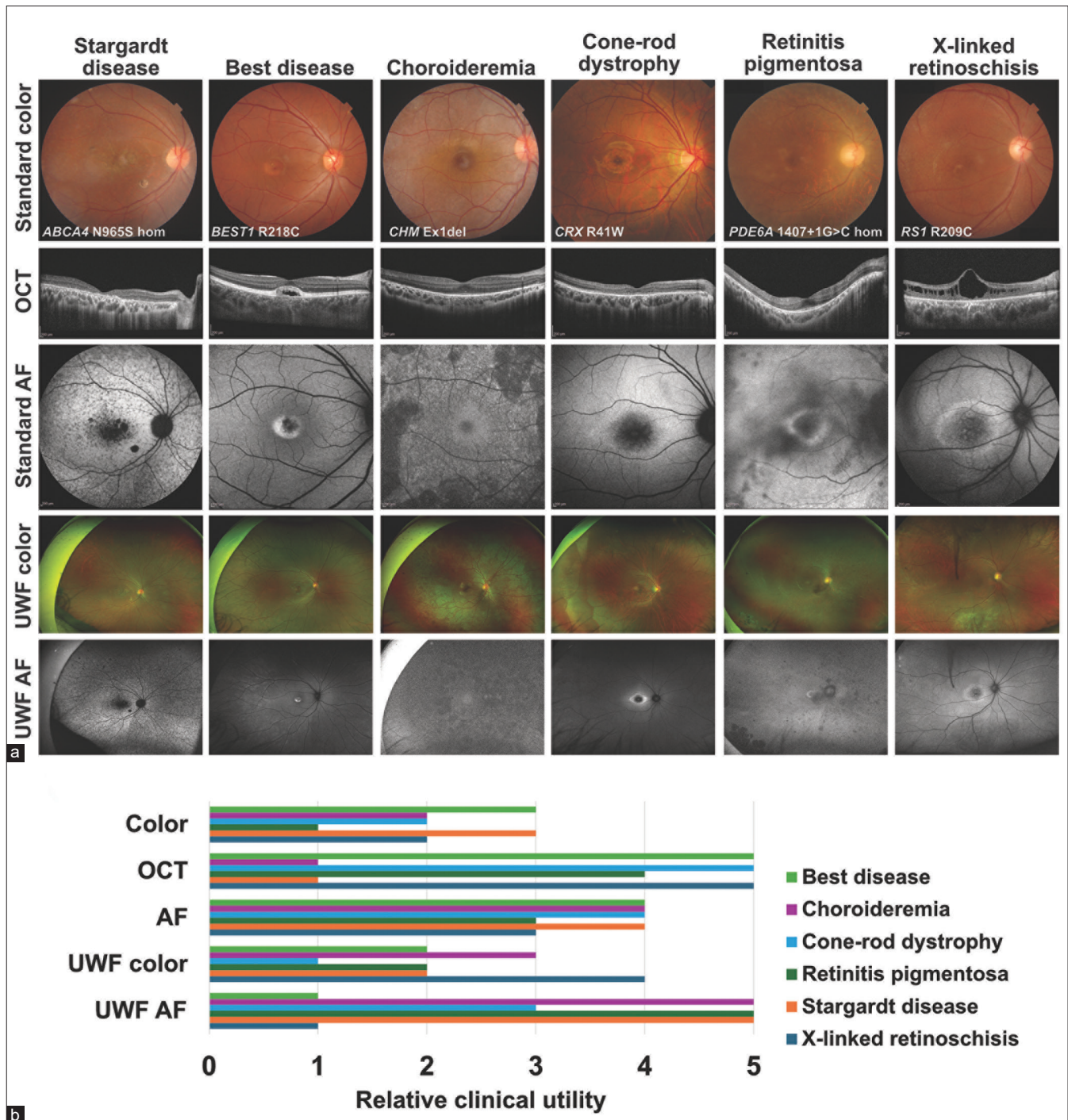


**Figure 4:** Comparison of the diagnostic utility of retinal imaging modalities in inherited retinal degeneration (IRD). (a) Six common IRD phenotypes are displayed with each of the most widely employed imaging modalities, including standard 40°–50° fundus color photography, macular spectral domain-optical coherence tomography, macular or standard field AF, ultra-widefield (UWF) color, and UWF AF imaging. Diagnostically helpful features for the cases shown include (1) hyper-AF flecks extending into the periphery with peripapillary sparing and macular atrophy in Stargardt disease; (2) subfoveal fluid with a hyper-AF signal in Best disease; (3) nummular or lobular hypo-AF signals extending into the periphery in choroideremia; (4) localized subfoveal outer retinal loss and central hypo-AF signals in cone-rod dystrophy; (5) diffuse peripheral hypo-AF with macular sparing and parafoveal outer retinal loss in RP; and (6) inner retinal macular schisis and peripheral schisis in X-linked retinoschisis. Genotypes are shown inset in the color fundus photographs. (b) Suggested clinical diagnostic utility for each imaging modality, when applied to each IRD phenotype, is shown with a relative ranking applied as a guide to highlight modalities that are helpful when phenotyping patients with suspected IRD

## Artificial Intelligence

The COVID-19 pandemic has bolstered research efforts in AI and its translation into healthcare. In

ophthalmology, ML and deep learning (DL) have drawn much interest and are the main drivers for AI-related research.<sup>[74,75]</sup> DL uses representation-learning methods with multiple levels of abstraction to process data



without manual feature engineering, which is in contrast to ML which is often labor intensive.<sup>[76]</sup> In a clinical context, DL automates the process of retinal image analysis and has been applied to CFP and OCT for the diagnosis and management of DR, glaucoma,

and AMD.<sup>[77-80]</sup> This method of DL has already been applied in a recent study on early retinal peripheral degeneration using DL detection of UWF-FP images with much success.<sup>[81]</sup> For IRD, DL offers the advantage of classification of IRDs, determining the genetic etiology as well as monitoring disease progression.<sup>[82,83]</sup> For example, Fujinami-Yokokawa *et al.* described the application of DL techniques to predict causative IRD genes of Stargardt disease (*ABCA4*), RP (*EYS*), and occult macular dystrophy (*RP1L1*) from CFP and FAF images with over 80% accuracy.<sup>[84]</sup> Chen *et al.* also developed a DL model for the early detection of RP with over 96% diagnostic accuracy compared to 81.5% by clinical ophthalmologists.<sup>[85]</sup> This is especially relevant where the diagnostic yield of IRD genotyping can be as low as 20%–40% in certain regional cohorts.<sup>[86,87]</sup> Charng *et al.* also developed a convolutional neural network algorithm that can monitor Stargardt disease progression through the progression of flecks on AF.<sup>[88]</sup> A recent study by quantified specific fundus AF features such as vessels and relative hypoautofluorescence across over 45,000 images from over 3,600 IRD patients using an AI model, and it appears likely that genotype-specific AF patterns, detected by AI-based approaches, will become an important biomarker for generating more accurate genetic hypotheses and solving IRD cases in future.<sup>[89]</sup>

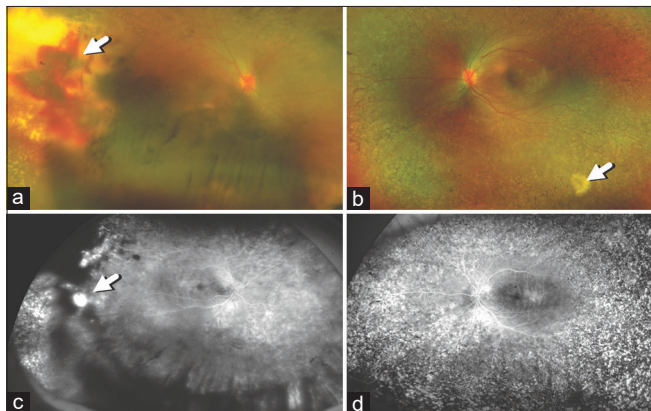


**Figure 5:** Ultra-widefield fluorescein angiography (Optos, MA, USA) findings in a 12-year-old female with RP and secondary vasoproliferative lesion with vitreous hemorrhage. (a) UWF pseudo-color image showing heavy exudation in the temporal periphery (arrow), accompanied by retinal hemorrhages and vitreous hemorrhage. (b) The fellow eye had bone spicule-like pigmentation and arteriolar attenuation, with a small vascular lesion seen inferotemporally (arrow). (c) UWF FA of the right eye disclosed the presence of multiple areas of temporal leakage (arrow) that were used to guide laser ablation of the vasoproliferative lesion. (d) Minimal dye leakage was seen in the fellow eye lesion

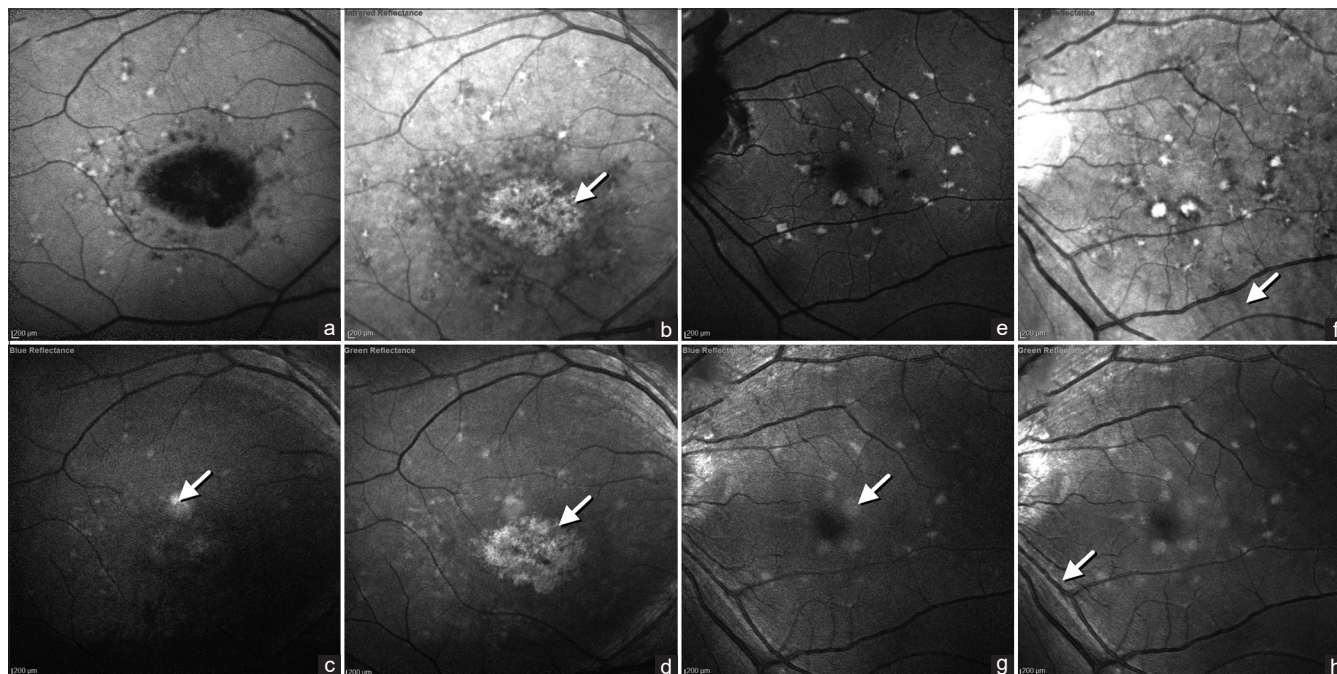


**Figure 6:** Multispectral imaging in patients with fleck retinal dystrophies. (a) AF imaging of a 66-year-old female with *ABCA4*-associated macular dystrophy, showing prominent central hypoautofluorescence with peripheral hyperautofluorescent flecks (b) Infrared reflectance shows central atrophy as a stippled hyperreflective area with surrounding hyporeflective foci, with hyperreflective flecks in the periphery. Fine detail is visible in the area of atrophy (arrow) which is less visible in the AF image. (c) Blue reflectance highlights the flecks, with early RPE changes (arrow) seen prior to its appearance in the AF image, while (d) green reflectance prominently highlights central RPE atrophy (arrow) and fleck-associated RPE atrophy as hyperreflectance. (e) AF imaging of a 61-year-old female with *PRPH 2*-associated macular dystrophy, which flecks highlighted as areas of hyperautofluorescence and fleck-associated RPE atrophy being hypoautofluorescent. (f) Infrared reflectance shows flecks as prominent hyperreflective foci and choroidal vessels (arrow), while (g) blue reflectance imaging highlights the flecks, albeit with lower contrast compared to AF and infrared reflectance. (h) Fine vascular detail is well visualized on green reflectance imaging (arrow) Images were captured using a Spectralis optical coherence tomography instrument (Heidelberg, Lübeck, Germany)



## Conclusion

The advancement of retinal imaging over the past few decades has revolutionized the IRD landscape through the introduction of novel imaging modalities and the enhancement of existing ones. With the plethora of imaging modalities already available today, we have acquired new knowledge on the pathophysiology of IRDs which facilitates earlier diagnosis and targeted genetic testing, monitoring of disease progression as well as guiding clinical trials for IRD therapeutics.

## Data availability statement

All data generated or analyzed during this study are included in this published article.

## Financial support and sponsorship

This study was supported by the SingHealth Foundation (grant R1748/71/2020; BJF) and the National Precision Medicine Programme phase II funding (MOH-000588; WKL).

## Conflicts of interest

The authors declare that there are no conflicts of interests of this paper.

## References

1. RetNet: Summaries. Available from: <https://web.sph.uth.edu/RetNet/sum-dis.htm?csrt=4951722033144288290#A-genes>. [Last accessed on 2024 Mar 03].
2. Chay J, Tang RW, Tan TE, Chan CM, Mathur R, Lee BJ, *et al*. The economic burden of inherited retinal disease in Singapore: A prevalence-based cost-of-illness study. *Eye (Lond)* 2023;37:3827-33.
3. Stone EM, Andorf JL, Whitmore SS, DeLuca AP, Giacalone JC, Streb LM, *et al*. Clinically focused molecular investigation of 1000 consecutive families with inherited retinal disease. *Ophthalmology* 2017;124:1314-31.
4. Liu X, Tao T, Zhao L, Li G, Yang L. Molecular diagnosis based on comprehensive genetic testing in 800 Chinese families with non-syndromic inherited retinal dystrophies. *Clin Exp Ophthalmol* 2021;49:46-59.
5. Wang L, Zhang J, Chen N, Wang L, Zhang F, Ma Z, *et al*. Application of whole exome and targeted panel sequencing in the clinical molecular diagnosis of 319 Chinese families with inherited retinal dystrophy and comparison study. *Genes (Basel)* 2018;9:360.
6. Pontikos N, Arno G, Jurkute N, Schiff E, Ba-Abbad R, Malka S, *et al*. Genetic basis of inherited retinal disease in a molecularly characterized cohort of more than 3000 families from the United Kingdom. *Ophthalmology* 2020;127:1384-94.
7. Weisschuh N, Obermaier CD, Battke F, Bernd A, Kuehlewein L, Nasser F, *et al*. Genetic architecture of inherited retinal degeneration in Germany: A large cohort study from a single diagnostic center over a 9-year period. *Hum Mutat* 2020;41:1514-27.
8. Perea-Romero I, Gordo G, Iancu IF, Del Pozo-Valero M, Almoquera B, Blanco-Kelly F, *et al*. Genetic landscape of 6089 inherited retinal dystrophies affected cases in Spain and their therapeutic and extended epidemiological implications. *Sci Rep* 2021;11:1526.
9. Shalom S, Ben-Yosef T, Sher I, Zag A, Rotenstreich Y, Poleg T, *et al*. Nationwide prevalence of inherited retinal diseases in the Israeli population. *JAMA Ophthalmol* 2024;142:609-16.
10. Heath Jeffery RC, Mukhtar SA, McAllister IL, Morgan WH, Mackey DA, Chen FK. Inherited retinal diseases are the most common cause of blindness in the working-age population in Australia. *Ophthalmic Genet* 2021;42:431-9.
11. Liew G, Michaelides M, Bunce C. A comparison of the causes of blindness certifications in England and Wales in working age adults (16-64 years), 1999-2000 with 2009-2010. *BMJ Open* 2014;4:e004015.
12. Georgiou M, Robson AG, Fujinami K, de Guimarões TA, Fujinami-Yokokawa Y, Daich Varela M, *et al*. Phenotyping and genotyping inherited retinal diseases: Molecular genetics, clinical and imaging features, and therapeutics of macular dystrophies, cone and cone-rod dystrophies, rod-cone dystrophies, Leber congenital amaurosis, and cone dysfunction syndromes. *Prog Retin Eye Res* 2024;100:101244.
13. Lam BL, Leroy BP, Black G, Ong T, Yoon D, Trzupek K. Genetic testing and diagnosis of inherited retinal diseases. *Orphanet J Rare Dis* 2021;16:514.
14. Fenner BJ, Whitmore SS, DeLuca AP, Andorf JL, Daggett HT, Luse MA, *et al*. A retrospective longitudinal study of 460 patients with ABCA4-associated retinal disease. *Ophthalmology* 2024;131:985-97.
15. Franceschetti A, Dieterle P. Diagnostic and prognostic importance of the electroretinogram in tapetoretinal degeneration with reduction of the visual field and hemeralopia. *Confin Neurol* 1954;14:184-6.
16. Marmor MF, Zrenner E. Standard for clinical electro-oculography. International society for clinical electrophysiology of vision. *Arch Ophthalmol* 1993;111:601-4.
17. Goodman G, Ripps H, Siegel IM. Cone dysfunction syndromes. *Arch Ophthalmol* 1963;70:214-31.
18. Testa F, Bacci G, Falsini B, Iarossi G, Melillo P, Mucciolo DP, *et al*. Voretigene neparvovec for inherited retinal dystrophy due to RPE65 mutations: a scoping review of eligibility and treatment challenges from clinical trials to real practice. *Eye (Lond)* 2024;38:2504-15.
19. Buch PK, Bainbridge JW, Ali RR. AAV-mediated gene therapy for retinal disorders: From mouse to man. *Gene Ther* 2008;15:849-57.
20. Fenner BJ, Tan TE, Barathi AV, Tun SB, Yeo SW, Tsai AS, *et al*. Gene-based therapeutics for inherited retinal diseases. *Front Genet* 2021;12:794805.
21. Ng DS, Lai TY, Ng TK, Pang CP. Genetics of bietti crystalline dystrophy. *Asia Pac J Ophthalmol (Phila)* 2016;5:245-52.
22. Rossi A, Rahimi M, Le D, Son T, Heiferman MJ, Chan RV, *et al*. Portable widefield fundus camera with high dynamic range imaging capability. *Biomed Opt Express* 2023;14:906-17.
23. Midenia E, Marchione G, Di Giorgio S, Rotondi G, Longhin E, Frizziero L, *et al*. Ultra-wide-field fundus photography compared to ophthalmoscopy in diagnosing and classifying major retinal diseases. *Sci Rep* 2022;12:19287.
24. Hirano T, Imai A, Kasamatsu H, Kakihara S, Toriyama Y, Murata T. Assessment of diabetic retinopathy using two ultra-wide-field fundus imaging systems, the Clarus® and Optos™ systems. *BMC Ophthalmol* 2018;18:332.
25. Georgiou M, Fujinami K, Michaelides M. Retinal imaging in inherited retinal diseases. *Ann Eye Sci* 2020;5:25.
26. Antaki F, Coussa RG, Kahwati G, Hammamji K, Sebag M, Duval R. Accuracy of automated machine learning in classifying retinal pathologies from ultra-widefield pseudocolour fundus images. *Br J Ophthalmol* 2023;107:90-5.
27. Wang NK, Fine HF, Chang S, Chou CL, Cella W, Tosi J, *et al*. Cellular origin of fundus autofluorescence in patients and mice with a defective NR2E3 gene. *Br J Ophthalmol* 2009;93:1234-40.
28. Pichi F, Abboud EB, Ghazi NG, Khan AO. Fundus autofluorescence

- imaging in hereditary retinal diseases. *Acta Ophthalmol* 2018;96:e549-61.
29. Brar M, Kozak I, Cheng L, Bartsch DU, Yuson R, Nigam N, *et al.* Correlation between spectral-domain optical coherence tomography and fundus autofluorescence at the margins of geographic atrophy. *Am J Ophthalmol* 2009;148:439-44.
  30. Antropoli A, Arrigo A, Bianco L, Cavallari E, Bandello F, Battaglia Parodi M. Hyperautofluorescent ring pattern in retinitis pigmentosa: Clinical implications and modifications over time. *Invest Ophthalmol Vis Sci* 2023;64:8.
  31. Sengillo JD, Lee W, Nagasaki T, Schuerch K, Yannuzzi LA, Freund KB, *et al.* A distinct phenotype of eyes shut homolog (EYS)-retinitis pigmentosa is associated with variants near the C-terminus. *Am J Ophthalmol* 2018;190:99-112.
  32. Chan CM, Tan TE, Jain K, Bylstra Y, Mathur RS, Tang RW, *et al.* Retinitis pigmentosa associated with the eys C2139Y VARIANT: An important cause of blindness in East Asian populations. *Retina* 2023;43:1788-96.
  33. Fenner BJ, Tan TE, Barathi AV, Tun SBB, Yeo SW, Tsai ASH, *et al.* Gene-Based Therapeutics for Inherited Retinal Diseases. *Front Genet* 2021;12:794805.5.
  34. Patal R, Banin E, Batash T, Sharon D, Levy J. Ultra-widefield fundus autofluorescence imaging in patients with autosomal recessive retinitis pigmentosa reveals a genotype-phenotype correlation. *Graefes Arch Clin Exp Ophthalmol* 2022;260:3471-8.
  35. Drexler W, Fujimoto JG. State-of-the-art retinal optical coherence tomography. *Prog Retin Eye Res* 2008;27:45-88.9.
  36. Adhi M, Liu JJ, Qavi AH, Grulkowski I, Lu CD, Mohler KJ, *et al.* Choroidal analysis in healthy eyes using swept-source optical coherence tomography compared to spectral domain optical coherence tomography. *Am J Ophthalmol* 2014;157:1272-81.e1.
  37. Witkin AJ, Ko TH, Fujimoto JG, Chan A, Drexler W, Schuman JS, *et al.* Ultra-high resolution optical coherence tomography assessment of photoreceptors in retinitis pigmentosa and related diseases. *Am J Ophthalmol* 2006;142:945-52.
  38. Hariri AH, Zhang HY, Ho A, Francis P, Weleber RG, Birch DG, *et al.* Quantification of ellipsoid zone changes in retinitis pigmentosa using en face spectral domain-optical coherence tomography. *JAMA Ophthalmol* 2016;134:628-35.
  39. Aizawa S, Mitamura Y, Baba T, Hagiwara A, Ogata K, Yamamoto S. Correlation between visual function and photoreceptor inner/outer segment junction in patients with retinitis pigmentosa. *Eye (Lond)* 2009;23:304-8.
  40. Yung M, Klufas MA, Sarraf D. Clinical applications of fundus autofluorescence in retinal disease. *Int J Retina Vitreous* 2016;2:12.
  41. Fenner BJ, Jamshidi F, Bhuyan R, Fortenbach CR, Jin HD, Boyce TM, *et al.* Vitreoretinal procedures in patients with inherited retinal disease. *Ophthalmol Retina* 2024;8:307-9.
  42. Swanson EA, Munro RJ, Ambrosio L, Bowe TS, Moskowitz A, Hansen RM, *et al.* Monitoring X-linked retinoschisis (XLR5) by Optical coherence tomography (OCT). *Invest Ophthalmol Vis Sci* 2016;57:4269.
  43. Fenner BJ, Russell JF, Drack AV, Dumitrescu AV, Sohn EH, Russell SR, *et al.* Long-term functional and structural outcomes in X-linked retinoschisis: Implications for clinical trials. *Front Med (Lausanne)* 2023;10:1204095.
  44. Cideciyan AV, Jacobson SG. Leber congenital amaurosis (LCA): Potential for improvement of vision. *Invest Ophthalmol Vis Sci* 2019;60:1680-95.
  45. Jin Y, Li S, Jiang Z, Sun L, Huang L, Zhang T, *et al.* Genotype-phenotype of CRB1-associated early-onset retinal dystrophy: Novel insights on retinal architecture and therapeutic window for clinical trials. *Invest Ophthalmol Vis Sci* 2024;65:11.
  46. Tan TE, Tang RW, Chan CM, Mathur RS, Fenner BJ. Diagnostic challenges in ABCA4-associated retinal degeneration: One gene, many phenotypes. *Diagnostics (Basel)* 2023;13:3530.
  47. Daich Varela M, Esener B, Hashem SA, Cabral de Guimaraes TA, Georgiou M, Michaelides M. Structural evaluation in inherited retinal diseases. *Br J Ophthalmol* 2021;105:1623-31.
  48. Hara A, Nakazawa M, Saito M, Suzuki Y. The qualitative assessment of optical coherence tomography and the central retinal sensitivity in patients with retinitis pigmentosa. *PLoS One* 2020;15:e0232700.
  49. Aizawa S, Mitamura Y, Hagiwara A, Sugawara T, Yamamoto S. Changes of fundus autofluorescence, photoreceptor inner and outer segment junction line, and visual function in patients with retinitis pigmentosa. *Clin Exp Ophthalmol* 2010;38:597-604.
  50. Ouyang Y, Heussen FM, Keane PA, Sadda SR, Walsh AC. The retinal disease screening study: Prospective comparison of nonmydriatic fundus photography and optical coherence tomography for detection of retinal irregularities. *Invest Ophthalmol Vis Sci* 2013;54:1460-8.
  51. Greig EC, Duker JS, Waheed NK. A practical guide to optical coherence tomography angiography interpretation. *Int J Retin Vitreous* 2020;6:1-17.
  52. Hope-Ross M, Yannuzzi LA, Gragoudas ES, Guyer DR, Slakter JS, Sorenson JA, *et al.* Adverse reactions due to indocyanine green. *Ophthalmology* 1994;101:529-33.
  53. Patel RC, Gao SS, Zhang M, Alabduljalil T, Al-Qahtani A, Weleber RG, *et al.* Optical coherence tomography angiography of choroidal neovascularization in four inherited retinal dystrophies. *Retina* 2016;36:2339-47.
  54. Koyanagi Y, Murakami Y, Funatsu J, Akiyama M, Nakatake S, Fujiwara K, *et al.* Optical coherence tomography angiography of the macular microvasculature changes in retinitis pigmentosa. *Acta Ophthalmol* 2018;96:e59-67.
  55. Battaglia Parodi M, Cicinelli MV, Rabiolo A, Pierro L, Gagliardi M, Bolognesi G, *et al.* Vessel density analysis in patients with retinitis pigmentosa by means of optical coherence tomography angiography. *Br J Ophthalmol* 2017;101:428-32.
  56. Alnawaiseh M, Schubert F, Heiduschka P, Eter N. Optical coherence tomography angiography in patients with retinitis pigmentosa. *Retina* 2019;39:210-7.
  57. Oh R, Bae K, Yoon CK, Park UC, Park KH, Lee EK. Quantitative microvascular analysis in different stages of retinitis pigmentosa using optical coherence tomography angiography. *Sci Rep* 2024;14:4688.
  58. Ong SS, Patel TP, Singh MS. Optical coherence tomography angiography imaging in inherited retinal diseases. *J Clin Med* 2019;8:2078.
  59. Inoue M, Jung JJ, Balaratnasingam C, Dansingani KK, Dhrami-Gavazi E, Suzuki M, *et al.* A comparison between optical coherence tomography angiography and fluorescein angiography for the imaging of type 1 neovascularization. *Invest Ophthalmol Vis Sci* 2016;57:T314-23.
  60. Magliyah M, Alshamrani AA, Schatz P, Taskintuna I, Alzahrani Y, Nowilaty SR. Clinical spectrum, genetic associations and management outcomes of coats-like exudative retinal vasculopathy in autosomal recessive retinitis pigmentosa. *Ophthalmic Genet* 2021;42:178-85.
  61. Zimmer C, Kahn D, Clayton R, Dugel P, Freund K. Innovation in diagnostic retinal imaging: Multispectral imaging. *Retina Today* 2014;9:94-9.
  62. Ma F, Yuan M, Kozak I. Multispectral imaging: Review of current applications. *Surv Ophthalmol* 2023;68:889-904.
  63. Dugel PU, Zimmer CN, Shahidi AM. A case study of choroideremia carrier – Use of multi-spectral imaging in highlighting clinical features. *Am J Ophthalmol Case Rep* 2016;2:18-22.
  64. Kubota R, Birch DG, Gregory JK, Koester JM. Randomised study evaluating the pharmacodynamics of emixustat hydrochloride in subjects with macular atrophy secondary to stargardt disease. *Br J Ophthalmol* 2022;106:403-8.
  65. Strauss RW, Muñoz B, Ho A, Jha A, Michaelides M, Cideciyan AV, *et al.* Progression of stargardt disease as determined by fundus



- autofluorescence in the retrospective progression of stargardt disease study (Progstar report No. 9). *JAMA Ophthalmol* 2017;135:123241.
66. Heath Jeffery RC, Thompson JA, Lo J, Lamey TM, McLaren TL, McAllister IL, *et al.* Atrophy expansion rates in stargardt disease using ultrawidefield fundus autofluorescence. *Ophthalmol Sci* 2021;1:100005.
  67. Pang CE, Suqin Y, Sherman J, Freund KB. New insights into stargardt disease with multimodal imaging. *Ophthalmic Surg Lasers Imaging Retina* 2015;46:25761.
  68. Marshall PJ, Treu T, Melbourne J, Gavazzi R, Bundy K, Ammons SM, *et al.* Superresolving distant galaxies with gravitational telescopes: Keck laser guide star adaptive optics and hubble space telescope imaging of the lens system SDSS J0737+3216. *Astrophys J* 2007;671:1196.
  69. Gill JS, Moosajee M, Dubis AM. Cellular imaging of inherited retinal diseases using adaptive optics. *Eye (Lond)* 2019;33:168398.
  70. Nakatake S, Murakami Y, Funatsu J, Koyanagi Y, Akiyama M, Momozawa Y, *et al.* Early detection of cone photoreceptor cell loss in retinitis pigmentosa using adaptive optics scanning laser ophthalmoscopy. *Graefes Arch Clin Exp Ophthalmol* 2019;257:116981.
  71. Jacque L, Duncan, Yuhua Zhang, Jarel Gandhi, Chiaki Nakanishi, Mohammad Othman, Kari E. H. Branham, Anand Swaroop, Austin Roorda; High-Resolution Imaging with Adaptive Optics in Patients with Inherited Retinal Degeneration. *Invest. Ophthalmol. Vis. Sci.* 2007;48:3283-91.
  72. Roorda A, Sundquist S, Solovyev A, Ratnam K, Lujan BJ, Stone EM, *et al.* Adaptive optics imaging reveals supernormal cone density in enhanced Scone syndrome. *Invest Ophthalmol Vis Sci* 2010;51:2934.
  73. Park SP, Hong IH, Tsang SH, Lee W, Horowitz J, Yzer S, *et al.* Disruption of the human cone photoreceptor mosaic from a defect in NR2E3 transcription factor function in young adults. *Graefes Arch Clin Exp Ophthalmol* 2013;251:2299309.
  74. Ting DS, Peng L, Varadarajan AV, Keane PA, Burlina PM, Chiang MF, *et al.* Deep learning in ophthalmology: The technical and clinical considerations. *Prog Retin Eye Res* 2019;72:100759.
  75. Ting DS, Pasquale LR, Peng L, Campbell JP, Lee AY, Raman R, *et al.* Artificial intelligence and deep learning in ophthalmology. *Br J Ophthalmol* 2019;103:16775.
  76. Tey KY, Cheong EZ, Ang M. Potential applications of artificial intelligence in image analysis in cornea diseases: A review. *Eye Vis* 2024;11:120.
  77. Burlina PM, Joshi N, Pekala M, Pacheco KD, Freund DE, Bressler NM. Automated grading of age-related macular degeneration from color fundus images using deep convolutional neural networks. *JAMA Ophthalmol* 2017;135:11706.
  78. Li Z, He Y, Keel S, Meng W, Chang RT, He M. Efficacy of a deep learning system for detecting glaucomatous optic neuropathy based on color fundus photographs. *Ophthalmology* 2018;125:1199206.
  79. Gulshan V, Peng L, Coram M, Stumpe MC, Wu D, Narayanaswamy A, *et al.* Development and validation of a deep learning algorithm for detection of diabetic retinopathy in retinal fundus photographs. *JAMA* 2016;316:240210.
  80. Ting DS, Cheung CY, Lim G, Tan GS, Quang ND, Gan A, *et al.* Development and validation of a deep learning system for diabetic retinopathy and related eye diseases using retinal images from multiethnic populations with diabetes. *JAMA* 2017;318:221123.
  81. Wu T, Ju L, Fu X, Wang B, Ge Z, Liu Y. Deep learning detection of early retinal peripheral degeneration from ultrawidefield fundus photographs of asymptomatic young adult (1719 years) candidates to airforce cadets. *Transl Vis Sci Technol* 2024;13:1.
  82. Miere A, Le Meur T, Bitton K, Pallone C, Semoun O, Capuano V, *et al.* Deep learning-based classification of inherited retinal diseases using fundus autofluorescence. *J Clin Med* 2020;9:3303.
  83. FujinamiYokokawa Y, Ninomiya H, Liu X, Yang L, Pontikos N, Yoshitake K, *et al.* Prediction of causative genes in inherited retinal disorder from fundus photography and autofluorescence imaging using deep learning techniques. *Br J Ophthalmol* 2021;105:12729.
  84. FujinamiYokokawa Y, Pontikos N, Yang L, Tsunoda K, Yoshitake K, Iwata T, *et al.* Prediction of causative genes in inherited retinal disorders from spectraldomain optical coherence tomography utilizing deep learning techniques. *J Ophthalmol* 2019;2019:1691064.
  85. Chen TC, Lim WS, Wang VY, Ko ML, Chiu SI, Huang YS, *et al.* Artificial intelligence-assisted early detection of retinitis pigmentosa – The most common inherited retinal degeneration. *J Digit Imaging* 2021;34:94858.
  86. Jiman OA, Taylor RL, Lenassi E, Smith JC, Douzgou S, Ellingford JM, *et al.* Diagnostic yield of panel-based genetic testing in syndromic inherited retinal disease. *Eur J Hum Genet* 2020;28:57686.
  87. BrittenJones AC, Gocuk SA, Goh KL, Huq A, Edwards TL, Ayton LN. The diagnostic yield of next generation sequencing in inherited retinal diseases: A systematic review and metaanalysis. *Am J Ophthalmol* 2023;249:5773.
  88. Charng J, Xiao D, Mehdizadeh M, Attia MS, Arunachalam S, Lamey TM, *et al.* Deep learning segmentation of hyperautofluorescent fleck lesions in stargardt disease. *Sci Rep* 2020;10:16491.
  89. Woof W, de Guimarões TAC, Al-Khuzaei S, Daich Varela M, Sen S, Bagga P, *et al.* Quantification of Fundus Autofluorescence Features in a Molecularly Characterized Cohort of More Than 3500 Inherited Retinal Disease Patients from the United Kingdom. *medRxiv* 2024:2024.03.24.24304809. doi: 10.1101/2024.03.24.24304809.